Received 13 November 2025; Accepted 28 November 2025
https://doi.org/10.48612/letters/2025-4-440-448
https://elibrary.ru/qbjjvw

Effect of complex alloying on the phase composition and oxidation resistance of O-Ti_2AlNb based intermetallic alloys

V. M. Imayev†1, D. M. Trofimov[1], A. A. Ganeev[1], R. R. Timiryaev[1], R. I. Zainullin[1],
M. R. Shagiev[1], J. Shen[2], R. R. Mulyukov[1]

†vimayev@mail.ru

[1]Institute for Metals Superplasticity Problems of the Russian Academy of Sciences, Ufa 450001, Russia
[2]Department of Materials Science and Engineering, Fujian University of Technology, Fuzhou, Fujian 350108, China

Abstract: The effect of complex alloying on the phase composition and oxidation resistance of intermetallic alloys based on the Ti_2AlNb phase has been studied. The following experimental alloys (in at.%) were investigated: Ti-22Al-25Nb-0.15B, Ti-22Al-21Nb-5.5(Zr, Mo, Ta, Sn, Hf)-0.3Si-0.15B, Ti-25Al-21Nb-5.5(Zr, Mo, Ta, Sn, Hf)-0.3Si-0.15B, Ti-23.5Al-23Nb-4(Zr, Mo, Ta, Hf)-0.3Si and Ti-23Al-25.5Nb-2.5(Zr, Mo)-0.3Si. The first alloy was used as a reference alloy. The complex alloys were alloyed with metallic elements having a high melting point and/or a higher atomic radius in order to improve oxidation and creep resistance, and to provide solid solution strengthening in a wide temperature range. The ratio between Al content and β-stabilization (in Mo-equivalent) of the alloying elements varied around the ratio value corresponding to the ternary Ti-22Al-25Nb alloy. As-cast alloys were annealed at 900°C followed by furnace cooling in order to thermodynamically equilibrate the as-cast ingots. The alloys based on Ti-22Al, Ti-23Al and Ti-23.5Al consisted mostly of two basic phases, O(Ti_2AlNb) and β/B2, whereas the complex alloy based on Ti-25Al was near completely single-phase and contained only insignificant amount of the β/B2 phase. The volume fraction of the β/B2 phase in the alloys containing 22 – 23.5 Al was in the range of 17.6 – 27.5%. Microalloying with boron led to formation of borides but did not refine the as-cast microstructure. DSC analysis showed that for all alloys, the equilibrium phase transformation sequence is as follows: $L \rightarrow \beta/B2 \rightarrow \beta/B2 + \alpha_2(Ti_3Al) \rightarrow \beta/B2 + \alpha_2(Ti_3Al) + O(Ti_2AlNb) \rightarrow O(Ti_2AlNb) + \beta/B2$. The oxidation behavior was evaluated for the annealed conditions of the alloys at 700°C/600 h. The oxidation resistance increased due to complex alloying, with an increase in the aluminum content and with a decrease in the β/B2 phase content. The highest oxidation resistance showed the alloys based on Ti-25 and 23.5Al. In these alloys, the mass gain after oxidation at 700°C/600 h was around 0.5 mg/cm^2. Potential advantages of the complex alloying of O-Ti_2AlNb based alloys are discussed.

Keywords: intermetallic O-Ti_2AlNb alloys, complex alloying, microstructure, oxidation resistance

Acknowledgements: *The financial support of the Ministry of Science and Higher Education of Russian Federation under grant No. 13.2251.21.0285 is highly appreciated. The work was performed using the facilities of the shared services center "Structural and Physical-Mechanical Studies of Materials" of the Institute for Metals Superplasticity Problems of the Russian Academy of Sciences.*

1. Introduction

The orthorhombic Ti_2AlNb phase was discovered by Banerjee in a Ti-25 at.% Al-12.5 at.% Nb alloy in 1988 [1]. This gave rise to the development of O-Ti_2AlNb alloys based on the intermetallic compound Ti_2AlNb [2, 3]. Ti_2AlNb-based alloys, known as O-phase based alloys, have superior high-temperature capability compared to titanium alloys and can potentially be used at operating temperatures up to 700°C instead of nickel-based superalloys [2 – 5]. Due to lower density (typically 5.2 – 5.4 g/cm^3), the O-Ti_2AlNb based alloys can reduce weight by nearly 40% without compromising mechanical strength compared to nickel-based superalloys.

Based on the varying ratios of Ti, Al and Nb, ternary O-Ti_2AlNb based alloys with some degree of conventionality can be classified into two generations [3, 6]. The first-generation O-Ti_2AlNb based alloys contain less than 25 at.% of Nb and consist of β/B2, $\alpha_2(Ti_3Al)$ and O(Ti_2AlNb) phase, such as Ti-22Al-23Nb [7, 8]. The $\alpha_2(Ti_3Al)$ phase is brittle and the presence of this phase can significantly compromise the ductility of Ti_2AlNb-based alloys [9,10]. The second-generation O-Ti_2AlNb based alloys contain not less than about 25 at.% of Nb and predominantly consist of O(Ti_2Al)Nb and β/B2 phase, such as Ti-22Al-25Nb and Ti-22Al-27Nb [11–14]. Both phases, O-Ti_2AlNb and β/B2, have enough slip systems and the second-generation O-Ti_2AlNb based alloys typically exhibit appreciably better room-temperature ductility and fracture toughness than γ-TiAl based alloys. At the same time, O-Ti_2AlNb based alloys are significantly inferior to γ-TiAl based alloys in terms of creep and oxidation resistance and, as is believed, cannot replace γ-TiAl alloys, for example, as a material for low pressure turbine (LPT) blades. However, is everything really so hopeless for O-Ti_2AlNb based alloys compared to the γ-TiAl based alloys?

It is known that the ternary Ti-(22 – 25)Al-(25 – 27)Nb (at.%) alloys of the second-generation are alloyed with elements such as Mo, W, V, Zr, Ta, Si in order to enhance strength, creep and oxidation resistance [4,15 –19]. In so doing, to preserve the two-phase O + β/B2 composition, the ratio between Al content (α-stabilization) and β-stabilization of the alloying elements apparently must be near the same as in the ternary Ti-(22 – 25)Al-(25 – 27)Nb alloys. However, this idea was not realized in the case of complex alloying of the O-Ti_2AlNb based alloy. Besides, despite decades of development, it seems that the choice of alloying elements has not been optimized taking into account their physical and chemical properties. The complex alloying can be apparently aimed at simultaneously enhancement of oxidation resistance, strength and creep resistance without significant compromising the room-temperature ductility. It is worth noting that two-phase O(Ti_2AlNb) + β/B2 alloys can demonstrate a very high ductility (δ = 22.7– 25% at room temperature) after forging [20, 21] or selective laser melting [22]. In both cases, this was due to a fine-grained structure, which was reached via recrystallization in the first case and extremely rapid cooling in the second case. Meanwhile, this suggests that complex alloying combined with forging or selective laser melting followed by heat treatment can provide quite acceptable room temperature ductility and higher strength and creep/oxidation resistance compared to the ternary Ti-(22 – 25)Al-(25 – 27)Nb alloys. In other words, acceptable ductility and enhanced high-temperature properties can result from a tailored microstructure and complex alloying, respectively. Thus, complex alloying is expected to bring the properties of O-Ti_2AlNb based alloys closer to those of γ-TiAl alloys. To achieve this goal, the following approaches to alloying second-generation O-Ti_2AlNb based alloys were proposed in the present work:

i) in the designed alloy, the ratio of the Al content and the β-stabilization effect due to alloying must be approximately the same as in ternary Ti-(22 – 25)Al-(25 – 27)Nb alloys. As mentioned, this is required to maintain the two-phase O + β/B2 composition and thus to ensure acceptable ductility;

ii) it is desirable that the alloying elements have a high melting point and/or a larger atomic radius compared to Nb, Ti, and Al. The first is favorable for creep/oxidation resistance through slowing diffusivity, while the latter enhances strength and creep resistance via solid solution strengthening;

iii) the alloying elements must have good solubility in the intermetallic phases O(Ti_2AlNb) and β/B2 excluding the formation of additional phases;

iv) a higher aluminum content (within the above-mentioned range) is preferable for increasing oxidation resistance [16];

v) microalloying with boron seems to be useful for refining the as-cast structure [23];

vi) microalloying with silicon is desirable for dispersion strengthening and oxidation resistance.

Table 1 shows the most appropriate alloying elements according to the proposed approaches. It is known that Zr, Mo, W, Ta and Hf, which are being *d*-elements, substitute for Ti and Nb sites also belonging to the *d*-block of chemical elements, and Sn being a *p*-element substitutes for Al belonging to the same *p*-block of chemical elements. Zr, Hf and Sn have larger atomic radii than Ti and Nb that should be favorable for solid solution strengthening. Mo, W, Ta and Hf have higher melting points that should increase the creep and oxidation resistance. In particular, Zr, Mo and Si were shown to be beneficial for improving oxidation resistance of O-Ti_2AlNb based alloys [4, 24]. Note also that Zr, Ta, Hf and Sn had a strong positive influence on creep and oxidation resistance in the case of γ-TiAl based alloys [25 – 29].

Table 1. Characteristics of elements most suitable for alloying O-Ti_2AlNb based alloys.

Chemical element	Atomic radius, nm	The melting point, °C	β-stabilizing effect (Mo-equivalent) [30, 31]
Ti	0.147	-	-
Al	0.143	-	-
Nb	0.146	2477	0.3
Zr	0.160	1855	near neutral
Mo	0.139	2623	1
W	0.137	3422	0.5
Ta	0.149	3017	0.25
Hf	0.159	2233	near neutral
Sn	0.162	232	near neutral

In the present work, Mo having a lower density than W was taken as a strong β-stabilizer. Zr, Ta, Hf and Sn or some of these elements were used as near-neutral (Zr, Hf, Sn) or weak (Ta) β-stabilizing alloying elements. Strictly speaking, Zr and Hf are weak β-stabilizing elements but their β-stabilizing effect is insignificant and therefore was not taken into account.

The purpose of the present work was to design the complex alloyed O-Ti_2AlNb based alloys following the proposed approaches for potential using as a blade material at operating temperatures up to 700°C. The ratio of the Al content and the β-stabilization varied depending on the alloying but remained in the same range as in the ternary alloys Ti-(22 – 25)Al-(25 – 27)Nb. This study focused on the phase composition and oxidation resistance of the new alloys. It should be emphasized that insufficient oxidation resistance is one of the main obstacles to the practical use of O-Ti_2AlNb based alloys. Potential advantages of the complex alloying of O(Ti_2AlNb) based alloys as applied to low pressure turbine blades are discussed.

2. Materials and experimental

Five O-Ti_2AlNb based alloys were taken as starting materials:
1) Ti-22Al-25Nb-0.15B (the reference alloy),
2) Ti-22Al-21Nb-5.5(Zr, Mo, Ta, Sn, Hf)-0.3Si-0.15B,
3) Ti-25Al-21Nb-5.5(Zr, Mo, Ta, Sn, Hf)-0.3Si-0.15B,
4) Ti-23.5Al-23Nb-4(Zr, Mo, Ta, Hf)-0.3Si and
5) Ti-23Al-25.5Nb-2.5 (Zr, Mo)-0.3Si (at.%)
(hereinafter, the alloys are designated as O-Ref, O-22, O-25, O-23.5 and O-23 alloy, respectively). Table 2 shows the alloy compositions in at.% and wt.%, as well as the alloy designations in the text.

The alloy ingots with an approximate size of ∅45 mm× ×16 mm were prepared by arc-melting in a Ti-gettered argon

Table 2. Alloy compositions and their designation in the text.

Alloy composition in at.%	Alloy composition in wt.%	Designation in the text
Ti-22Al-25Nb-0.15B	Ti-10.9Al-42.64Nb-0.03B	O-Ref
Ti-22Al-21Nb-5.5(Zr, Mo, Ta, Sn, Hf)-0.3Si-0.15B	Ti-10.48Al-34.44Nb-11.78(Zr, Mo, Ta, Sn, Hf)-0.03B-0.15Si	O-22
Ti-25Al-21Nb-5.5(Zr, Mo, Ta, Sn, Hf)-0.3Si-0.15B	Ti-12.04Al-34.82Nb-11.91(Zr, Mo, Ta, Sn, Hf)-0.03B-0.15Si	O-25
Ti-23.5Al-23Nb-4(Zr, Mo, Ta, Hf)-0.3Si	Ti-11.25Al-37.9Nb-8.92(Zr, Mo, Ta, Hf)-0.15Si	O-23.5
Ti-23Al-25.5Nb-2.5(Zr, Mo)-0.3Si	Ti-11.16Al-42.6Nb-4.2(Zr, Mo)-0.15Si	O-23

atmosphere. Only high purity starting elements were used. To ensure homogeneity of composition, the ingots were repeatedly turned over and remelted. Energy-dispersive X-Ray spectroscopy (EDS) confirmed the nominal compositions of ingots. The alloy compositions were also controlled by weighing the initial elements before casting and the resulting ingot. The mass loss was always not more than 0.1%.

Table 3 shows the Al content, the β-stabilization (in Mo-equivalent) and the ratio of Al content (Al-equivalent) to Mo-equivalent calculated for the studied alloys. Zr and Sn were not taken into account for the Al-equivalent (because these elements are near neutral and their influence on the Al-equivalent is insignificant). Mo-equivalent was calculated by the following equation [30, 31]:

$$[Mo]_{eq} = \%Mo + \%Ta/4 + \%Nb/3.3 + \%W/2 + \%V/1.4 + \\ + \%Cr/0.6 + \%Mn/0.6 + \%Fe/0.4 + \%Ni/0.8 \quad (1)$$

where all concentrations are given in wt.%. The ratio of Al content and β-stabilization of the alloying elements varied around the ratio value corresponding to the reference alloy (Table 3).

To roughly estimate the effect of alloying on the cast structure, the macrostructures were prepared from the as-cast alloys. To do it, the cross sections of ingots were ground and etched using the etchant $15\%HNO_3 + 5\%HF + 80\%$ distilled water. To achieve thermodynamic equilibrium, the as-cast alloys were annealed at a temperature of 900°C (2 h) followed by slow furnace cooling.

Microstructure examination was carried out by scanning electron microscopy (SEM) in the back-scattering electron (BSE) mode in a Tescan Mira-3 microscope equipped with EDS. Before study, the specimen surfaces were mechanically and electrolytically polished. BSE images were used to evaluate the volume fraction of the β/B2 phase after annealing at 900°C (2 h). To do it, the contrast was increased in the BSE images, thus highlighting the β/B2 phase.

The cast and annealed alloys were investigated by differential scanning calorimetry (DSC). DSC runs were performed with a heating rate of 20°C/min under pure Ar using a heat flux calorimeter Jupiter STA 449 F1 Netzsch. To identify the phase composition of the alloys, X-ray diffraction (XRD) analysis was carried out for the annealed alloys at room temperature using a DRON-4 diffractometer and Cu-K_α radiation. The software product X'Pert HighScore Plus was used to indicate the phase compositions of the alloys.

Table 3. Al content, β-stabilization due to alloying and the ratio of the Al content and β-stabilization for the O-Ti_2AlNb based alloys under study.

Alloy	Al content, wt.%	β-stabilization (Mo-equivalent)	The Al/Mo-eq ratio
O-Ref	10.9	12.92	0.84
O-22	10.48	12.93	0.81
O-25	12.04	13.07	0.92
O-23.5	11.25	13.99	0.8
O-23	11.16	14.98	0.74

Five samples (one sample per alloy) with a size of 20 mm × 12 mm × 1 mm were cut by spark cutting from the ingots after annealing at 900°C (2 h). All surfaces of the samples were ground down to a 4000 grit using SiC paper. Before oxidation experiment, the samples were cleaned with ethanol, washed with distilled water and dried in air. The samples were isothermally exposed in a furnace at 700°C for 600 h with periodic inspection and weighing on an analytical balance with an accuracy of 10^{-6} g. The oxide spallation was not observed during oxidation and only an increase in mass of the samples occurred, which was detected by periodic weighing of the samples.

The dependences of the mass gain $\Delta M = \Delta m/S$ (in mg/cm²), where Δm is the increase in weight and S is the surface area, and the mass gain rate on time were obtained. The mass gain per unit area ($\Delta M = \Delta m/S$) is usually described by the following power-law equation [4]:

$$(\Delta M)^n = k \times t \quad (2)$$

n is the power exponent, k is the oxidation rate constant (in $mg^n \times cm^{-2n} \times h^{-1}$) and t is the oxidation time. For the obtained dependencies of $\Delta M(t)$, regression analysis was carried out using Eq. (2) and the software product SigmaPlot 12.5. The fitting curves and calculated equations based on Eq. (2) were plotted and the n and k values were defined.

3. Results and discussion

Figure 1 shows the macrostructures of the alloys in the as-cast conditions. One can see that the coarser macrostructure was obtained in the reference alloy, while slightly finer macrostructures were reached in the O-22, O-25, O-23.5 and O-23 alloy. This means that complex alloying reduces the prior β grain size. It is interesting that despite doping with boron, the macrostructures of the reference alloy, the O-22 and O-25 alloy were coarse-grained. The prior β grain size reached up to 5 – 7 mm in the reference alloy, up to 1 – 2 mm in O-22 and O-25, and up to 2 – 2.5 mm in O-23.5 and O-23 (Fig. 1). Thus, the macrostructures were coarse-grained regardless of boron microalloying. This indicates that borides formed during melting and freezing were not effective in reducing the prior β grain size. It should be noted that in the case of β-solidifying γ-TiAl based alloys microalloying with

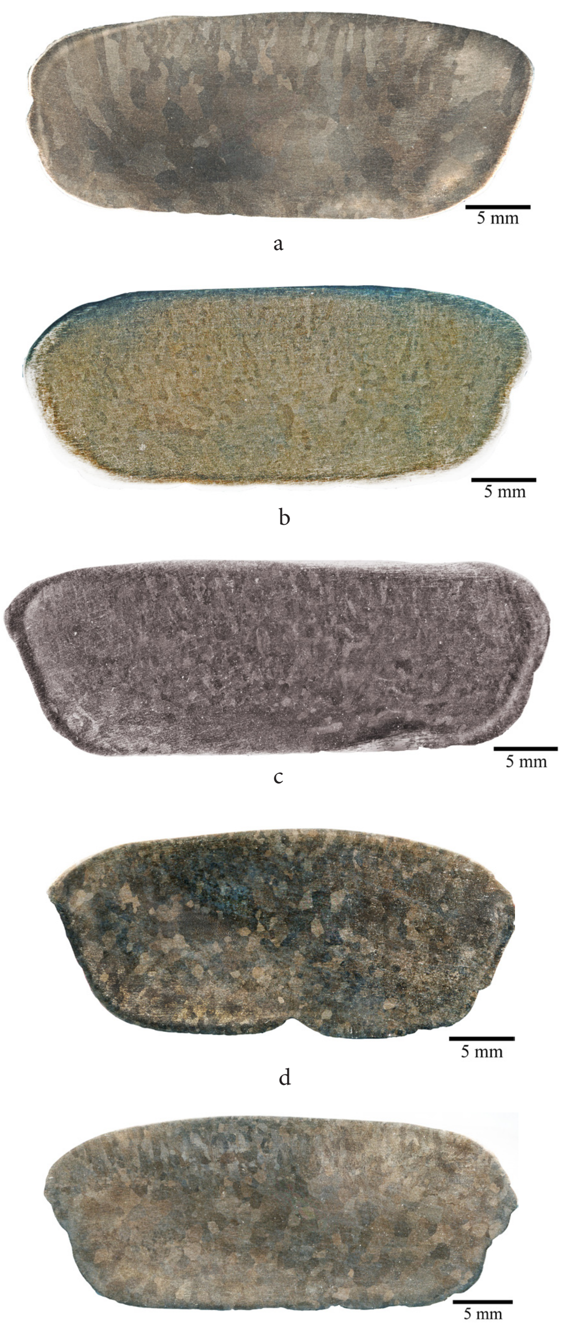

Fig. 1. (Color online) Macrostructures of ingots in as-cast conditions: O-Ref (a), O-22 (b), O-25 (c), O-23.5 (d), O-23 (e).

0.1–0.2 at.% boron proved to be very effective in refining the cast structure [28,29,32]. The preservation of a large size of the prior β grains in the O-Ti_2AlNb based alloys can be explained by the high crystallization temperature and incomplete transformation of the β phase during freezing and cooling of ingots.

Figure 2 shows the XRD patterns obtained for the alloys in the cast and annealed conditions. For alloys containing 22–23.5 Al and having the Al/Mo-eq ratio of 0.74–0.84, the peaks of the O(Ti_2AlNb) and β/B2 phases were detected, whereas for the alloy containing 25 Al and having the Al/Mo-eq ratio of 0.92 only peaks corresponding to the O(Ti_2AlNb) phase were detected. It should be emphasized that in all alloys, the peaks of the α_2(Ti_3Al) phase were not detected.

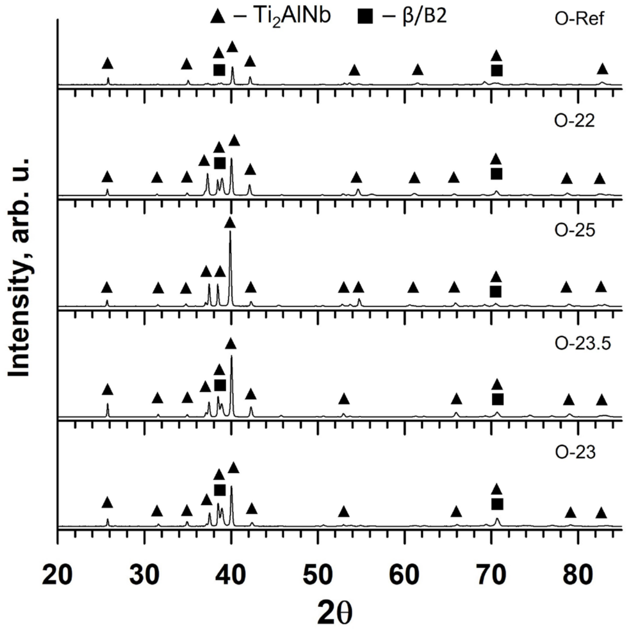

Fig. 2. XRD patterns obtained for the alloys in the cast and annealed conditions.

Figure 3 represents the BSE images of alloys in the cast and annealed conditions. The alloys containing 22–23.5 Al have a typical two-phase structure consisting of O(Ti_2AlNb) and β/B2 phase, whereas the alloy containing 25 Al looks as near completely single-phase alloy. Apparently, the O-25 alloy contained only a very small amount of the β/B2 phase (having a light contrast), which was not detected by XRD analysis.

Table 4 indicates the phase compositions of the alloys in the cast and annealed conditions. The volume fraction of the β/B2 phase in the alloys containing 22–23.5 Al varied in the range of 17.6–27.5%. Among alloys containing 22–23.5 Al the highest content of the β/B2 phase was observed in the O-Ref alloy (27.5%) and the lowest content (17.6%) in the O-22 alloy. It is interesting that the volume fraction of the β/B2 phase not exactly correlated with the Al/Mo-eq ratio. Apparently, the phase composition of the O-Ti_2AlNb based alloys also depends on the heat treatment conditions and Nb content [15,33].

Figure 4 shows the heat flow curves obtained as a result of DSC measurements of alloys in the cast and annealed conditions. The obtained DSC traces were very similar for all two-phase alloys based on Ti-(22–23.5)Al despite some differences in the Al/Mo-eq ratio. The DSC curve obtained for the O-25 alloy turned out to be different. This can be explained by the almost single-phase composition due to the significantly higher Al/Mo-eq ratio. For all alloys, the equilibrium phase transformation sequence is as follows: L → β/B2 → β/B2+α_2(Ti_3Al) → β/B2+α_2(Ti_3Al)+O(Ti_2AlNb)→ → O(Ti_2AlNb) + β/B2.

It should be noted that the ordering of the β phase (β → B2) was observed in all alloys during annealing at 900°C (2 h) followed by furnace cooling. This was revealed through DSC measurements of alloys in the as-cast conditions (not presented here), which showed exothermic effect at around

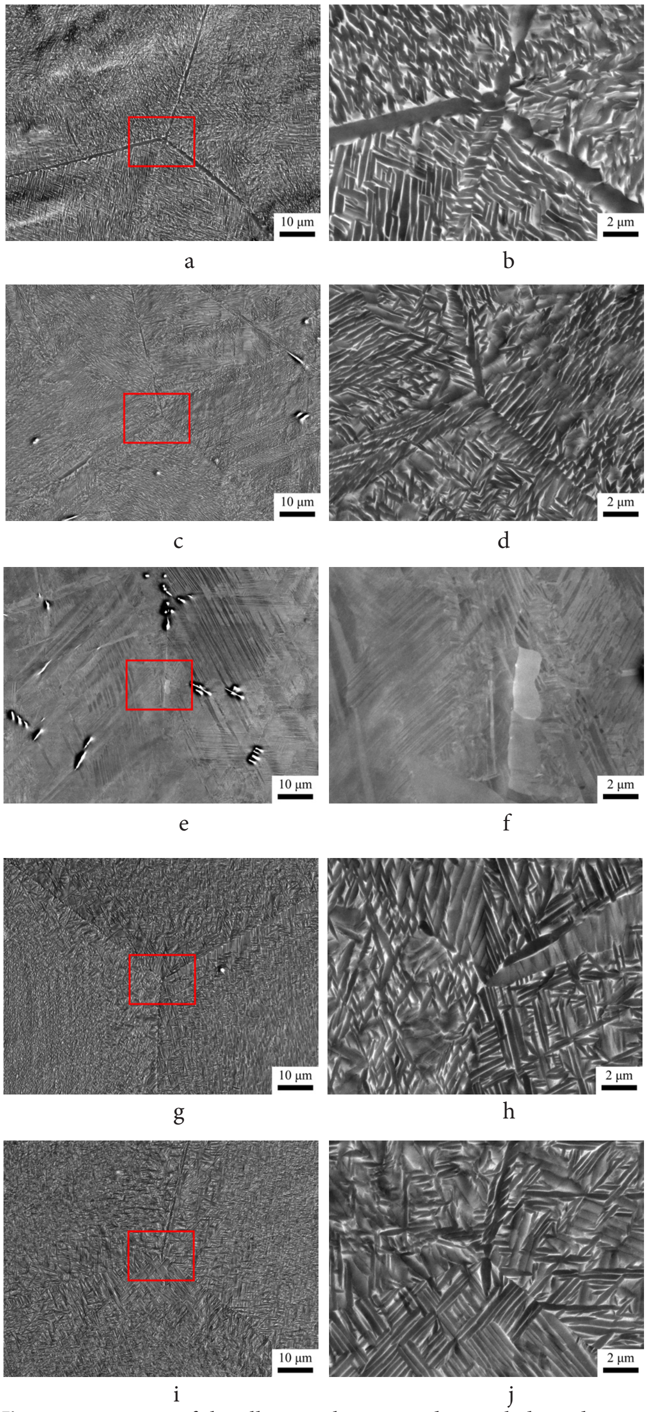

Fig. 3. BSE images of the alloys in the cast and annealed conditions: O-Ref (a,b), O-22 (c,d), O-25 (e,f), O-23.5 (g,h), O-23 (i,j). In (a,c,e,g,i), the areas are indicated from which the images (b,d,f,h,j) were obtained at a higher magnification.

700°C. Annealing of cast alloys at 900°C led to disappearance of this exothermic effect caused by ordering of the β phase. Note that this is consistent with the pseudo-binary phase diagram based on Ti-22Al-*x*Nb [3,34]. In the temperature range of 1160–1300°C, both exothermic and endothermic phenomenon were observed, which is most likely associated with the ordering of the β and disordering of the B2 phase, respectively.

According to [34,35], the ordered B2 phase with a space group of *Pm3m* can transform to the disordered β phase with *Im3m* space group at higher temperatures, as well as tend to

Table 4. The phase compositions of the alloys in the cast and annealed conditions.

Alloy	The volume fractions of O(Ti_2AlNb) / β/B2, %	The Al/Mo-eq ratio
O-Ref	72.5 / 27.5	0.84
O-22	82.4 / 17.6	0.81
O-25	>99 / <1	0.92
O-23.5	80.5 / 19.5	0.8
O-23	79.3 / 20.7	0.74

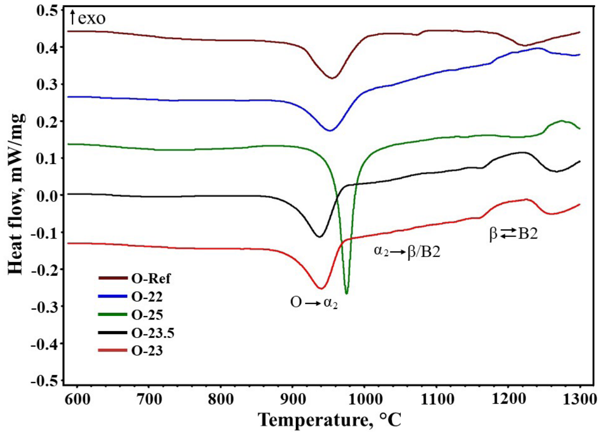

Fig. 4. (Color online) Heat flow curves obtained as a result of DSC measurements of the alloys in the cast and annealed conditions.

decompose into disordered β phase below 750°C. Our DSC measurements suggest that rapid cooling of ingots led to the formation of disordered β phase, while annealing of as-cast ingots at 900°C (that corresponds to the two- or three-phase region, see below Table 5) followed by slow furnace cooling resulted in ordering of the β phase. In other words, rapid cooling is a possible reason for the disordering of the B2 phase below 750°C. DSC measurements also revealed that at higher temperatures both disordering of the B2 phase, causing an endothermic effect, and ordering of the β phase, causing an exothermic effect, can occur. The latter statement, however, requires further experimental confirmation.

Table 5 indicates the temperature ranges corresponding to the various phase regions. The $\alpha_2 \rightarrow \beta$/B2 transformation is apparently accompanied by a very weak thermal effect, and further quenching experiments followed by XRD measurements are required to verify the determined temperature ranges (in particular, the β-transus). Nevertheless, the obtained temperature ranges are more or less consistent with currently available literature data, in particular with pseudo-binary phase diagrams based on Ti-22Al-*x*Nb and Ti-25Al-*x*Nb [3,15,33,34,36,37].

Figure 5 displays the mass gain curves drawn as fitting curves based on Eq. (2) and corresponding to the calculation equations obtained for samples of the O-Ti_2AlNb based alloys isothermally exposed in air at 700°C for 600 hours. The mass gain after 600 h of holding increased for alloy samples in the following sequence: O-25, O-23.5, O-23, O-22 and O-Ref. This indicates that oxidation resistance increases primarily with increasing Al content, which is consistent with [16]. Owing to a higher Al content, the O-23.5 and

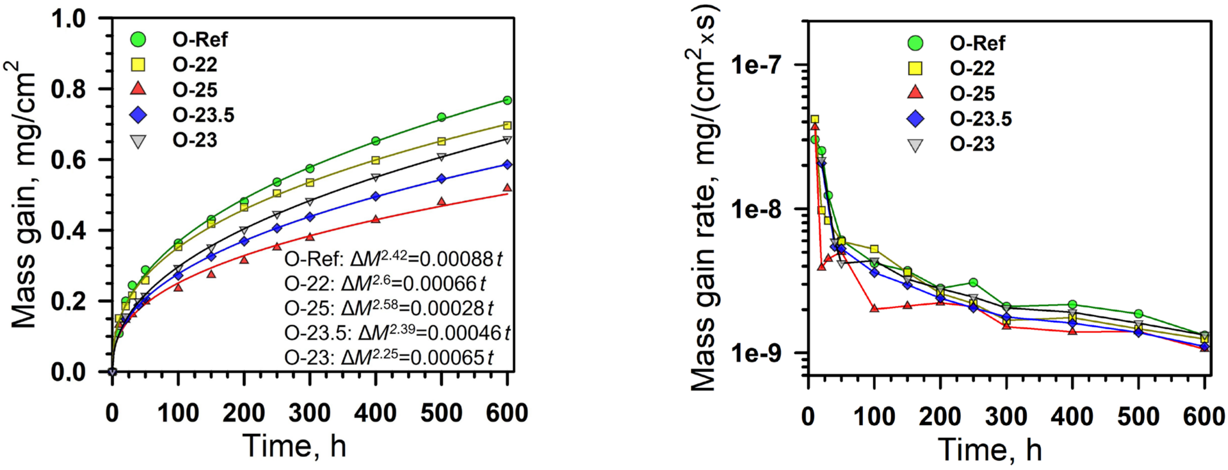

a b

Fig. 5. (Color online) The mass gain curves drawn using regression analysis (a) and the time dependencies of the mass gain rate (b) obtained for samples of the O-Ti_2AlNb based alloys isothermally exposed in air at 700°C/600 h.

Table 5. Temperature ranges corresponding to different phase regions in the alloys under study.

Phase region	The alloy and temperature range, °C
O(Ti_2AlNb) + β/B2	O-Ref: <913.1°C O-22: <908.5°C O-25: <959°C O-23.5: <899°C O-23: <898.2°C
β/B2 + α_2(Ti_3Al) + O(Ti_2AlNb)	O-Ref: 913.1 – 997.5°C O-22: 908.5 – 995.4°C O-25: 959 – 989.3°C O-23.5: 899.0 – 966.9°C O-23: 898.2 – 967.5°C
β/B2 + α_2(Ti_3Al)	O-Ref: 997.5 – 1083.4°C O-22: 995.4 – 1031.6°C O-25: 989.3 – 1130°C O-23.5: 966.9 – 1077.1°C O-23: 967.5 – 1033.7°C
β/B2	O-Ref: >1083.4°C O-22: >1031.6°C O-25: >1130°C O-23.5: >1077.1°C O-23: >1033.7°C

O-23 alloy showed higher oxidation resistance than the O-22 alloy. The fact that the O-23.5Al alloy demonstrated higher oxidation resistance than the O-23Al alloy suggests that complex alloying (including Ta, Hf) contributed to the increase in oxidation resistance despite the higher Nb content in the O-23 alloy compared to the O-23.5 alloy (25.5 against 23 at.%). Note that Nb is known to bring a beneficial effect on the oxidation resistance in TiAl based alloy by inhibiting the oxygen diffusion and reducing rutile growth rate [38,39]. However, β-stabilizing effect of Nb should be apparently also taken into account in the case of the O-Ti_2AlNb based alloys. Most likely that the higher β/B2 content decreased the oxidation resistance. It is one of the reasons, why the reference alloy showed the worst oxidation resistance among the alloys under study despite a higher Nb content (25 at.%). Another reason of lower oxidation resistance of the O-Ref alloy is the lack of complex alloying. Note that borides formed during melting and freezing apparently had no noticeable effect on oxidation resistance.

Thus, complex alloying has a complex influence on the phase composition and oxidation resistance. As follows from the results obtained, the main factors affecting the oxidation resistance of the O-Ti_2AlNb based alloys are the following: i) increasing the Al content significantly improves oxidation resistance, which can be associated with the formation of protective Al_2O_3. This is consistent with [16]; ii) the orthorhombic phase based on Ti_2AlNb has a higher oxidation resistance than the β/B2 phase [3]; iii) complex alloying, particularly with refractory metals such Ta, Mo and Hf, results in an increase in oxidation resistance through most likely slowing down diffusivity and an increase in microstructural stability. At the same time, further investigations of oxidation products depending on alloying are required to clarify this issue.

Figure 5b shows the time dependencies of the rate of mass gain. In all alloys, with increasing holding time, the rate of mass gain gradually decreased and became weakly dependent on time. This indicates that oxidation products formed during exposure gradually reduced the penetration of oxygen and nitrogen into the material. One can conclude that theoretical curves based on Eq. (2) agreed well with the experimental mass gain curves. Thus, the oxidation kinetics of the studied alloys obeys quasi-parabolic laws with different values of n and k. The power exponents and oxidation rate constants of the alloys are listed in Table 6. For comparison, these parameters are also given for the Ti-(23 – 24)Al-(21 – 22)Nb-(1.5 – 2)Mo-(1 – 1.5)Zr-(0.2 – 0.3)Si alloy [4]. A higher value of n and a lower value of k indicate slower oxidation kinetics.

In Table 6, the predicted mass gain values after 1000 h (according to the calculated quasi-parabolic laws) are also shown. As after 600 h of holding, the mass gain increased for alloy samples in the following sequence: O-25, O-23.5, O-23, O-22 and O-Ref. It is worth noting that all alloys under study

Table 6. The power exponent *n*, the oxidation rate constant *k*, and predicted mass gain after exposure at 700°C/1000 h obtained for the O-Ti_2AlNb based alloys based on Eq. (2).

Alloy	*n*	*k* ($mg^n \times cm^{-2n} \times h^{-1}$)	Predicted mass gain after 1000 h, mg/cm^2
O-Ref	2.42	8.8×10^{-4}	0.95
O-22	2.6	6.6×10^{-4}	0.853
O-25	2.58	2.8×10^{-4}	0.613
O-23.5	2.39	4.6×10^{-4}	0.726
O-23	2.25	6.5×10^{-4}	0.826
Ti-(23-24)Al-(21-22)Nb-(1.5-2)Mo-(1-1.5)Zr-(0.2-0.3)Si [4]	2 2	1.6×10^{-3} 4.2×10^{-4}	1.3* (700°C/1000 h) 0.67* (650°C/1000 h)

* These are experimental results, which were taken from ref. [4].

showed higher oxidation resistance compared to that of the Ti-(23–24)Al-(21–22)Nb-(1.5–2)Mo-(1–1.5)Zr-(0.2–0.3)Si alloy after exposure at 700°C/1000 h [4]. One can see that the oxidation resistance of the O-25 and O-23.5 alloys after holding at 700°C/1000°C was very close to that of the Ti-(23–24)Al-(21–22)Nb-(1.5–2)Mo-(1–1.5)Zr-(0.2–0.3)Si alloy after holding at 650°C/1000 h. This means that the approaches proposed in the introduction allowed us to improve the oxidation resistance by about 50°C.

Thus, the O-Ti_2AlNb based alloys under study can be considered as oxidation-resistant materials (obeying the quasi-parabolic law with different values of *n* and *k*), in which diffusion-controlled scale growth occurred when held at 700°C. From the viewpoint of a benchmark value assumed for evaluation of the oxidation resistance of TiAl alloys [40], the samples of all alloys under study showed acceptable oxidation resistance (less than 1 mg/cm^2 after 1000 h exposure at 700°C). It is clear that the O-25 alloy is unlikely to be considered for practical applications due to its low O(Ti_2AlNb) phase content and presumably low ductility. However, the O-23.5 and O-23 alloys, containing about 20 vol.% of the β/B2 phase, can certainly be considered as promising candidates for practical applications at temperatures up to 700°C without surface treatment or protective coating against oxidation. In particular, the O-23.5 and O-23 alloys can be used as materials for manufacturing of LPT blades for gas turbine engines. As mentioned in the introduction, complex alloying is to improve oxidation and creep resistance, while strength and ductility will be achieved through careful microstructural control. It seems that the latter can be reached through selective laser melting or hot forging providing microstructure refinement due to extremely rapid cooling [22] or dynamic recrystallization [20, 21], followed by solid solution heat treatment and ageing.

Thus, the idea of complex alloying taking into account the physical and chemical properties of the alloying elements, as well as the Al/Mo-eq ratio turned out to be very productive. Further investigations are to show, whether the complex alloyed alloy, such as O-23.5 or O-23, have improved strength, creep resistance at temperatures up to 700°C and acceptable ductility for practical use as a structural material.

4. Conclusions

The present work was devoted to the study of complex alloys based on O-Ti_2AlNb. Using complex alloying, we tried bring the properties of O-Ti_2AlNb based alloys closer to those of γ-TiAl alloys. The following main conclusions can be drawn:

– To reach a higher high-temperature capability in O-Ti_2AlNb based alloys the following alloy designing approaches are proposed: i) when alloying O-Ti_2AlNb based alloys, the physicochemical properties of the alloying elements must be taken into account. In particular, it is desirable for the alloying elements to have a high melting point and/or a larger atomic radius than Nb, Ti, and Al. The first is favorable for creep/oxidation resistance, while the latter expectedly enhances strength and creep resistance; ii) to maintain the desirable two-phase composition O + β/B2 (in order to maintain acceptable ductility), the ratio of the Al content and the β-stabilization effect due to alloying should be approximately the same as in the ternary Ti-22Al-25Nb alloy; iii) a higher aluminum content and microalloying with Si are preferable for increasing oxidation resistance.

– The obtained results showed that a higher Al content (23–23.5 at.%) and complex alloying with such elements as Zr, Mo, Ta, Hf and microalloying with Si significantly improves the oxidation resistance at 700°C, while ensuring the desirable two-phase O + β/B2 composition. In particular, the mass gain obtained for sample of the Ti-23.5Al-23Nb-4(Zr, Mo, Ta, Hf)-0.3Si(O-23.5) alloy after holding at 700°C/600 h was less than 0.6 mg/cm^2.

– The oxidation kinetics of the alloys during oxidation at 700°C/600 h obeyed the calculated quasi-parabolic laws. The mass gain values based on the quasi-parabolic laws were predicted after oxidation at 700°C/1000 h. For all the alloys studied, the mass gain after 1000 h of exposure was less than a benchmark value (1 mg/cm^2 after 1000 h holding) assumed for assessing the oxidation resistance. Particularly, for the Ti-23.5Al-23Nb-4(Zr, Mo, Ta, Hf)-0.3Si alloy this value was estimated as 0.726 mg/cm^2.

– Microalloying with boron was found to be not effective in microstructural refinement of as-cast ingots. This can be ascribed to high crystallization temperature and incomplete transformation of the β phase during freezing and cooling of ingots.

– Based on the experiments conducted, the designed new two-phase alloys based on O-Ti_2AlNb, containing 22–23.5 Al, in particular, the Ti-23.5Al-23Nb-4(Zr, Mo, Ta, Hf)-0.3Si alloy, can be considered for application as a structural material with operating temperature of up to 700°C without surface treatment or protective coating against oxidation.

References

1. D. Banerjee, A.K. Gogia, T.K. Nandi, V.A. Joshi, A new ordered orthorhombic phase in a Ti_3Al-Nb alloy, Acta Met. 36 (1988) 871–882.
2. D. Banerjee, The Intermetallic Ti_2AlNb. Prog. Mater. Sci. 42 (1997) 135–158.
3. R. Hu, K. Zhang, H. Zou, Z. Gao, X. Luo, X. Liu, Z. Wu, Research progress on Ti_2AlNb-based alloys and composites for aerospace applications, Journal of Alloys & Compounds, 1021 (2025) 179701.
4. M. Dade, V.A. Esin, L. Naze, P. Sallot, Short- and long-term oxidation behaviour of an advanced Ti_2AlNb alloy, Corrosion Science 148 (2019) 379–387.
5. Y. Huang, Y. Liu, Y. Zhang, H. Liang, Thermal stability and mechanical properties of Ti-22Al-25Nb alloy with different initial microstructures, Journal of Alloys & Compounds 842 (2020) 155794.
6. S. Liu, J. Cao, Y. Zhou, S. Dai, X. Huang, C. Cao, Research and prospect of Ti_2AlNb alloy, Chin. J. Nonferrous Met. 31 (2021) 3106–3126.
7. C.F. Yolton, J.P. Beckman, Powder metallurgy processing and properties of the ordered orthorhombic alloy Ti-22at.%Al-23at.%Nb, Mater. Sci. Eng. A. 192 (1995) 597–603.
8. W.A. Baeslack, P.S. Liu, P.R. Smith, J. Gould, Characterization of solid-state resistance welds in SiC-reinforced orthorhombic-based Ti-22Al-23Nb (at.%) titanium aluminide, Mater. Charact. 41 (1998) 41–51.
9. S. Emura, A. Araoka, M. Hagiwara, B2 grain size refinement and its effect on room temperature tensile properties of a Ti-22Al-27Nb orthorhombic intermetallic alloy, Scr. Mater. 48 (2003) 629–634.
10. C. Xue, W. Zeng, B. Xu, X. Liang, J. Zhang, S. Li, B2 grain growth and particle pinning effect of Ti-22Al-25Nb orthorhombic intermetallic alloy during heating process, Intermetallics 29 (2012) 41–47.
11. Y. Huang, Y. Liu, C. Li, Z. Ma, L. Yu, H. Li, Microstructure evolution and phase transformations in Ti-22Al-25Nb alloys tailored by super-transus solution treatment, Vacuum, 161 (2019) 209–219.
12. R.G. Rowe, US Patent No. 5032357, 1991.
13. J. Peng, Y. Mao, S. Li, X. Sun, Microstructure controlling by heat treatment and complex processing for Ti_2AlNb based alloys, Materials Science & Engineering, 299 (2001) 75–80.
14. S.J. Yang, S. Emura, S.W. Nam, M. Hagiwara, H.S. Jeon, S.B. Yoon, Improvement of creep resistance in TiB particle reinforced Ti_2AlNb composite particularly above 700°C, Materials Letters, 58 (2004) 3187–3191.
15. F. Tang, Sh. Nakazawa, M. Hagiwara, The effect of quaternary additions on the microstructures and mechanical properties of orthorhombic Ti_2AlNb-based alloys, Materials Science & Engineering A 329–331 (2002) 492–498.
16. L. Germann, D. Banerjee, J.Y. Guedou, J.-L. Strudel, Effect of composition on the mechanical properties of newly developed Ti_2AlNb-based titanium aluminide, Intermetallics 13 (2005) 920–924.
17. J. Yang, Q. Cai, Z. Ma, Y. Huang, L. Yu, H. Li, Y. Liu, Effect of W addition on phase transformation and microstructure of powder metallurgic Ti-22Al-25Nb alloys during quenching and furnace cooling, Chinese Journal of Aeronautics, 32 (2019) 1343–1351.
18. Y. Zhang, Y. Liu, L. Yu, H. Liang, Y. Huang, Z. Ma, Microstructures and tensile properties of Ti_2AlNb and Mo-modified Ti_2AlNb alloys fabricated by hot isostatic pressing, Materials Science and Engineering A 776 (2020), 139043.
19. N. Li, Z.B. Zhao, H. Sun, T.Y. Zhou, Q.J. Wang, J.X. Yang, Y.H. Liu, B.H. Zhang, Effects of heat treatment on microstructure evolution and mechanical properties of Ti-22Al-24Nb-0.5Mo alloy, Materials Science and Engineering A 857 (2022) 144052.
20. M.R. Shagiev, R.M. Galeyev, O.R. Valiakhmetov, R.V. Safiullin, Improved Mechanical Properties of Ti_2AlNb-Based Intermetallic Alloys and Composites, Adv. Mater. Res. 59 (2009) 105–108.
21. V.M. Imayev, R.M. Imayev, R.A. Gaisin, T.I. Nazarova, M.R. Shagiev, R.R. Mulyukov, Heat resistant intermetallic alloys and composites based on titanium: microstructure, mechanical properties and possible application, Materials Physics & Mechanics 33 (2017) 80–96. (in Russian)
22. Y. Zhou, W. Li, D. Wang, L. Zhang, K. Ohara, J. Shen, T. Ebel, M. Yan, Selective laser melting enabled additive manufacturing of Ti-22Al-25Nb intermetallic: excellent combination of strength and ductility, and unique microstructural features associated, Acta Mater. 173 (2019) 117–129.
23. F. Tang, Sh. Nakazawa, M. Hagiwara, Effect of boron microalloying on microstructure, tensile properties and creep behavior of Ti-22Al-20Nb-2W alloy, Materials Science and Engineering A 315 (2001) 147–152.
24. W. Dang, J.S. Li, T.B. Zhang, H.C. Kou, Oxidation behavior of Zr-containing Ti_2AlNb-based alloy at 800°C, Trans. Nonferrous Met. Soc. China 25 (2015) 783–790.
25. V.M. Imayev, R.M. Imayev, A.V. Kuznetsov, Mechanical Properties of Thermomechanically Treated Ti-rich $\gamma+\alpha_2$ Titanium Aluminide Alloys, Scripta Materialia, 49 (2003) 1047–1052.
26. D.M. Trofimov, V.M. Imayev, R.M. Imayev, The influence of alloying and microstructure on oxidation resistance of β-solidifying γ-TiAl alloys, Letters on Mater. 14 (4) (2024) 386–393.
27. D.M. Trofimov, V.M. Imayev, R.M. Imayev, Preliminary study of the effect of Sn addition on microstructure and creep resistance of a β-solidifying TiAl alloy, Intermetallics 169 (2024) 108310.
28. V.M. Imayev, D.M. Trofimov, R.M. Imayev, Microstructure, mechanical properties and oxidation resistance of intermetallic β-solidifying γ-TiAl based alloys, Intermetallics 176 (2025) 108556.
29. V.M. Imayev, D.M. Trofimov, R.M. Imayev, Influence of alloying with tantalum on microstructure, mechanical properties and oxidation resistance of an advanced β-solidifying γ-TiAl based alloy, Journal of Alloys and Compounds 1046 (2025) 184864.
30. Metallography of Titanium Alloys (ed. by N.F. Anoshkin), Moscow, Metallurgy, 1980, 464 p. (in Russian)

31. A. A. Ilyin, V. A. Kolachev, I. S. Polkin, Titanium alloys. Composition, structure, properties. Reference book, Moscow, VILS-MATI, 2009, 520 p. (in Russian)
32. H. Clemens, S. Mayer, Design, processing, microstructure, properties, and applications of advanced intermetallic TiAl alloys, Adv. Eng. Mater. 15 (2013) 191–215.
33. X. Chen, Z. Weidong, W. Wei, L. Xiaobo, Z. Jianwei, Quantitative analysis on microstructure evolution and tensile property for the isothermally forged Ti_2AlNb based alloy during heat treatment, Materials Science and Engineering A 573 (2013) 183–189.
34. C. J. Boehlert, B. S. Majumdar, V. Seetharaman, D. B. Miracle, Part I. The Microstructural Evolution in Ti-Al-Nb O+BCC Orthorhombic Alloys, Metallurgical & Materials Transactions A 30 (1999) 2305–2323.
35. C. J. Boehlert, The phase evolution and microstructural stability of an orthorhombic Ti-23Al-27Nb alloy, J. of Phase Equilibria 20 (1999) 101–108.
36. A. K. Gogia, T. K. Nandy, D. Banerjee, T. Carisey, J. L. Strudel, J. M. Franchet, Microstructure and mechanical properties of orthorhombic alloys in the TiAl-Nb system, Intermetallics 6 (1998) 741–748.
37. W. Wang, W. Zeng, C. Xue, X. Liang, J. Zhang, Microstructural evolution, creep, and tensile behavior of a Ti-22Al-25Nb (at%) orthorhombic alloy, Materials Science and Engineering A 603 (2014) 176–184.
38. M. Yoshihara, K. Miura, Effects of Nb addition on oxidation behavior of TiAl, Intermetallics 3 (1995) 357–363.
39. J. P. Lin, L. L. Zhao, G. Y. Li, L. Q. Zhang, X. P. Song, F. Ye, G. L. Chen, Effect of Nb on oxidation behavior of high Nb containing TiAl alloys, Intermetallics 19 (2011) 131–136.
40. R. Pflumm, S. Friedle, M. Schütze, Oxidation protection of γ-TiAl-based alloys — A review, Intermetallics 56 (2015) 1–14.